Supplementary material to the article: “Explicit Definitions for the Electromagnetic Energies in Electromagnetic Radiation”

Gaobiao Xiao, *Senior Member, IEEE*

This document is a supplementary material to the article submitted to IEEE Antennas and Propagation Magazine: “Explicit Definitions for the Electromagnetic Energies in Electromagnetic Radiation”. Readers can also access to a 50min video on IEEE TechRxiv: A Theory for Electromagnetic Radiation and Electromagnetic Coupling (techrxiv.org). The main revisions in version 4 are: (1) delete the part about mutual couplings; (2) changed some denotations, e.g., the primary radiative energy and primary radiative power are denoted respectively by $W_{rad}^{pri}(t)$ and $P_{rad}^{pri}(t)$;(3) added a reference [21] to show that potentials may be gauge invariant if they are subject to some conditions.

This document includes 6 parts: (1) background of the work. (2) the reason to introduce the macroscopic Schott energy. (3) detailed derivation of the explicit expressions for the energies of a pulse radiator in free space. (4) detailed derivation for the energies and powers of the Hertzian dipole. (5) explanation to the negative energy that may appear in sources like a loop current. (6) the numerical techniques used to calculate the energies.

1. Background of the Work

The reactive energy f an antenna has been investigated by many researchers, and the frequency domain calculation methods proposed so far can be roughly divided into two types:

(1) Methods in early stage, mainly based on spherical mode expansion technique [1]-[3].

- In 1948, Chu discussed in his paper [4] the radiation problem associated with electrically small antennas, and derived ladder type equivalent circuits for TM_{n0}/TE_{n0} spherical waves. The reactive energy only includes those stored in the reactive elements in the equivalent circuit, hence is bounded and can be accurately evaluated.
- Collin [1] calculated the reactive energies strictly with fields obtained using mode decomposition method [5][6], where the reactive energies of spherical modes and cylindrical modes are obtained by directly integrating the term $(\varepsilon_0/4)\mathbf{E}\cdot\mathbf{E}^*$and $(\mu_0/4)\mathbf{H}\cdot\mathbf{H}^*$ in the whole space outside a sphere with a small radius. Since the integration is infinite, the energy density associated with the radiation fields has to be subtracted from the integrand.
- Fante [2] extended the results of Collin, and McLean re-examined the case of small antennas and calculated the Q factors of TM_{10} and TE_{10} mode [3].

For small antennas, spherical mode expansion solution for reactive energy is a good approximation, and can provide satisfactory upper bound for Q factors. It has been extended to analyzing antennas with larger sizes [7], where the radiation fields by a current distribution are expanded with spherical modes. However, it is not efficient because a lot of modes may need to be taken into account for antennas with large size and complicated structures. Furthermore, the fields inside the sphere enclosing the antenna cannot be addressed accurately.

(2) Numerical methods investigated by many researchers [8]-[14].

The key problem is the total electromagnetic energy of an antenna is unbounded when it works in harmonic state because the total radiative energy of the antenna is unbounded, as the antenna is assumed to keep radiating in the whole timespan of $-\infty<t<+\infty$. However, there is no well-accepted method to separate the reactive energy and the radiative energy. An empirical strategy is to subtract an additional term of energy density associated with the radiation fields from the integrand. Unfortunately, the result is usually not the exact solution to the reactive electromagnetic energy, and the additional energy density is ultimately an ambiguous concept without a rigorous definition. Two representative formulations are the follows,

- Yaghjian and Best have adopted this method to calculate the Q factor of antennas [8]. They used the reactive theorem by Rhodes in [15], which can be simplified in free space as

$$|I_0|^2X_0'=\lim_{r\to\infty}\left\{\int_V \mathrm{Re}(\boldsymbol{B}\cdot\boldsymbol{H}^*+\boldsymbol{D}^*\cdot\boldsymbol{E})\,dV-r^2\,\mathrm{Im}\int_{4\pi}\left(\mathbf{E}\times\mathbf{H'}^*_{\mathrm{I}_0}-\mathbf{E}'\times\mathbf{H}^*_{\mathrm{I}_0}\right)\cdot\hat{\mathbf{r}}\mathrm{d}\Omega\right\} \quad (1)$$

where I_0 is the excitation current at the feeding port of the antenna. The primes stand for derivatives w.r.t ω, and X_0 is the input reactance at the feeding port when it is tuned with a series positive inductance or capacitance.

V is the spherical domain with radius r. The term $\int_V \mathrm{Re}(\boldsymbol{B}\cdot\boldsymbol{H}^*+\boldsymbol{D}^*\cdot\boldsymbol{E})\,dV$ is related to the conventionally defined electromagnetic energy. In Yaghjian-Best formulation, (1) is transformed into

$$|I_0|^2X_0' = \lim_{r\to\infty}\left\{\int_V Re(\boldsymbol{B}\cdot\boldsymbol{H}^*+\boldsymbol{D}^*\cdot\boldsymbol{E})\,dV - 2\varepsilon_0 r\int_{4\pi}F^2d\Omega + \frac{2}{\eta_0}Im\int_{4\pi}\boldsymbol{F}_{I_0}'\cdot\boldsymbol{F}^*d\Omega\right\} \quad (2)$$

where ε_0 and η_0 are respectively the permittivity and intrinsic impedance in free space, and $\boldsymbol{F}$ is the far electric field. The first two terms in RHS of (2) are considered as the reactive electromagnetic energy in Yaghjian-Best formulation, which is coordinate dependent,

$$W_F = \lim_{r\to\infty}\int_V Re(\boldsymbol{B}\cdot\boldsymbol{H}^*+\boldsymbol{D}^*\cdot\boldsymbol{E})\,dV - 2\varepsilon_0 r\int_{4\pi}F^2d\Omega \quad (3)$$

We have calculated the Q-factor of a grid antenna with W_F . When we choose the origin on the yellow circle, the Q-factor changes because W_F changes with the origin, as shown in Fig.1.

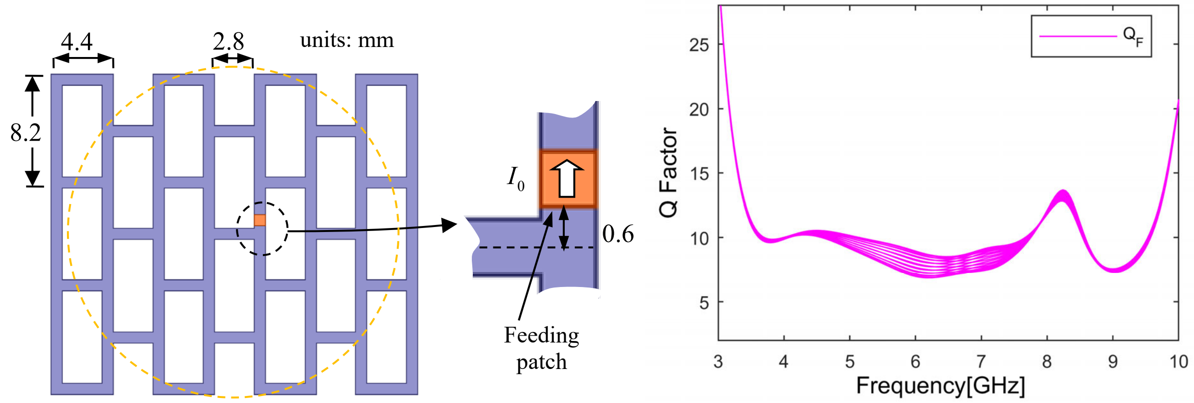

Fig. 1. Grid antenna. (a) Structure. (b) Q factor calculated with W_F .

- Vandenbosch [16] proposed a set of formulae for calculating the reactive energies, which are expressed in closed form of integrations with respect to the current densities in the antenna structure. In free space, the core equation Vandenbosch formulation, can be simplified as

$$-\frac{1}{2}\int_{V_s}\boldsymbol{E}'\cdot\boldsymbol{J}^*\,dV = P_{rad}' + j\left[\lim_{r\to\infty}\int_V Re(\boldsymbol{D}^*\cdot\boldsymbol{E}+\boldsymbol{B}\cdot\boldsymbol{H}^*)\,dV + 2W_{rad,G}\right] (4)$$

where the additional term is

$$W_{rad,G} = \lim_{r\to\infty} Im\frac{1}{4}\oint_S(\boldsymbol{E}'\times\boldsymbol{H}^*-\boldsymbol{E}\times\boldsymbol{H}'^*)\cdot\hat{\boldsymbol{n}}dS \quad (5)$$

In Vandenbosch formulation, $(-0.5W_{rad,G})$ is used as the additional term to replace the term associated with the radiation power. With this modification, the reactive energy can be directly computed with a set of closed-form expressions that are coordinate-independent. Gustafsson and Jonsson evaluated W_F analytically to get [17],

$$W_F = W_{van} + W_{F_2} \quad (6)$$

where $W_{van} = \left(W_{vac}^m + W_{vac}^e + W_{rad,\ G}\right)$ is the total reactive energy in Vandenbosch formulation, and W_{F_2} is a coordinate-dependent term.

Yaghjian-Best formulation and Vandenbosch formulation have attracted many attentions from researchers [18]-[23]. They have been successfully applied to analysis and optimization of small antennas [24]-[29]. The Vandenbosch formulation has been extended to time domain [30][31]. However, it is reported that the Vandenbosch formulation can produce negative values of stored energy for electrically large structures [28], which has not been satisfactorily explained. Furthermore, the formulation in time domain may give results that are a little bit different from those obtained with the formulation in frequency domain [31].

There are other methods to calculate the reactive energies [32]. A comprehensive comparison of them can be found in [22]. However, for those methods that require to evaluate the reactive energies, W_F and W_{van} are the most popular choices.

(3) Our formulation in frequency domain [33][34].

Since 2019, we have careful re-examined this issue and found that the difficulty involved in reactive energy can be traced back to an old classical problem: for a given time-varying current distribution $\mathbf{J}(\mathbf{r},t)$ in domain V_a, how to determine the reactive electromagnetic energy stored in the whole free space. We cut into this issue by focusing on the following two equations,

$$W_e = \int_{V_a} \frac{1}{2}\rho\phi d\boldsymbol{r}_1 = \int_{V_\infty} \frac{1}{2}\boldsymbol{E}\cdot\boldsymbol{D}\, d\boldsymbol{r}_1 \quad (7)$$

$$W_J(t) = \frac{1}{2}\int_{V_a} \boldsymbol{J}\cdot\boldsymbol{A} d\boldsymbol{r}_1 = \int_{V_\infty} \frac{1}{2}\boldsymbol{B}\cdot\boldsymbol{H}\, d\boldsymbol{r}_1 \quad (8)$$

It is easy to check that the second equation in (7) and (8) do not hold true for electro-dynamic fields. We argued that the two source-potential terms must be the correct definition for the reactive energies. Although we now believe that the choice is reasonable and is in consistent with their time domain formulation, we realized later that some of the discussions and statement are not rigorous or even not correct because of our superficial understanding to the issue at that time. For example, we did not clearly emphasize that the source-potential term is only for the reactive energy not the total electromagnetic energy. We tried to fix this in a conference paper [34], however, the formulation, together with the time domain formulation proposed in this article, are still regarded by some reviewers to be the same as the Carpenter formulation, or simply a static limit one. We have clarified in this article that they are not.

As is clear, the main difficulty in frequency domain formulation is due to the fact that the radiative energy of a harmonic source is unbounded. It is then natural to investigate the energy issue associated with a pulse radiator, as its radiative energy and the reactive energy should be finite, so is its total electromagnetic energy. As has discussed in the article, mainly two kinds of time domain formulations for this issue can be found in published literatures. Except that proposed by Vandenbosch [30][31], the other one was proposed by Shlivinski and Heyman [13][14], which is an approximate method. So we kept on considering on this issue in the past two years because we firmly believe that the issue is still of great significance to antenna society and should be solved. Moreover, we realized that the most important and essential case is the radiation problem in vacuum. If the electromagnetic energy issue in vacuum remains to be ambiguous, it is much more difficult to solve it when media are included. We finally get a satisfactory energy separation formulation in vacuum by introducing the macroscopic Schott energy, and verified that the formulation is in consistent to the frequency domain formulation that we have proposed 2 years ago. Meanwhile, the proposed theory can provide a better understanding of some ambiguous concepts in our previous versions of the formulation.

2. Why to Introduce Macroscopic Schott Energy

Consider in free space a radiator with charge density $\rho(\mathbf{r}_1,t)$ and $\mathbf{J}(\mathbf{r}_1,t)$, $\mathbf{r}_1 \in V_s$. From Maxwell equations, the electric energy density and the magnetic energy density can be transformed to

$$\frac{1}{2}\boldsymbol{D}\cdot\boldsymbol{E} = \frac{1}{2}\rho\phi - \frac{1}{2}\boldsymbol{D}\cdot\frac{\partial \boldsymbol{A}}{\partial t} - \frac{1}{2}\nabla\cdot(\boldsymbol{D}\phi) \quad (9)$$

$$\frac{1}{2}\boldsymbol{B}\cdot\boldsymbol{H} = \frac{1}{2}\boldsymbol{J}\cdot\boldsymbol{A} + \frac{1}{2}\frac{\partial \boldsymbol{D}}{\partial t}\cdot\boldsymbol{A} - \frac{1}{2}\nabla\cdot(\boldsymbol{H}\times\boldsymbol{A}) \quad (10)$$

where $\boldsymbol{E}$ and $\boldsymbol{H}$ are the electromagnetic fields, $\boldsymbol{D}$ and $\boldsymbol{B}$ are the flux densities. The scalar potential ϕ and the vector potential $\boldsymbol{A}$ are subject to the Lorentz Gauge and their reference zero points are put at the infinity. For a pulse radiator in $[0,T]$, the total electric energy and the total magnetic energy can be written as

$$W_{tot}^{e}(t) = \int_{V_\infty}\left(\frac{1}{2}\boldsymbol{D}\cdot\boldsymbol{E}\right)d\boldsymbol{r}_1 = \int_{V_s}\left(\frac{1}{2}\rho\phi\right)d\boldsymbol{r}_1 + \int_{V_\infty}\left(-\frac{1}{2}\boldsymbol{D}\cdot\frac{\partial \boldsymbol{A}}{\partial t}\right)d\boldsymbol{r}_1 - \oint_{S_\infty}\frac{1}{2}\phi\boldsymbol{D}\cdot\hat{\boldsymbol{n}}dS \quad (11)$$

$$W_{tot}^{m}(t) = \int_{V_\infty}\left(\frac{1}{2}\boldsymbol{B}\cdot\boldsymbol{H}\right)d\boldsymbol{r}_1 = \int_{V_s}\left(\frac{1}{2}\boldsymbol{J}\cdot\boldsymbol{A}\right)d\boldsymbol{r}_1 + \int_{V_\infty}\left(\frac{1}{2}\frac{\partial \boldsymbol{D}}{\partial t}\cdot\boldsymbol{A}\right)d\boldsymbol{r}_1 - \oint_{S_\infty}\frac{1}{2}(\boldsymbol{H}\times\boldsymbol{A})\cdot\hat{\boldsymbol{n}}dS \quad (12)$$

The surface integrals in the right hand side of (9) and (10) are zeros for pulse radiators because their fields never reach S_∞. Denote

$$W_\rho(t) = \int_{V_s}\frac{1}{2}\rho(\boldsymbol{r}_1,t)\phi(\boldsymbol{r}_1,t)\,d\boldsymbol{r}_1 \quad (13)$$

$$W_J(t) = \int_{V_s}\frac{1}{2}\boldsymbol{J}(\boldsymbol{r}_1,t)\cdot\boldsymbol{A}(\boldsymbol{r}_1,t)\,d\boldsymbol{r}_1 \quad (14)$$

$W_{\rho J} = W_\rho + W_J$ is the Coulomb-velocity energy. It is generally considered that the total electric/magnetic consists of an electric/magnetic radiative energy and an electric/magnetic reactive energy, namely,

$$W_{tot}^{e}(t) = W_{react}^{e}(t) + W_{rad}^{e}(t), \quad W_{tot}^{m}(t) = W_{react}^{m}(t) + W_{rad}^{m}(t) \quad (15)$$

If we define $W_{react}^{e}(t) = W_{\rho}(t)$, $\quad W_{react}^{m}(t) = W_{J}(t)$, then we have to admit that

$$W_{rad}^{e}(t) = W_{tot}^{e}(t) - W_{react}^{e}(t) = \int_{V_\infty} \left(-\frac{1}{2}\boldsymbol{D} \cdot \frac{\partial \boldsymbol{A}}{\partial t}\right) d\boldsymbol{r}_1 \quad (16)$$

$$W_{rad}^{m}(t) = W_{tot}^{m}(t) - W_{react}^{m}(t) = \int_{V_\infty} \left(\frac{1}{2}\frac{\partial \boldsymbol{D}}{\partial t} \cdot \boldsymbol{A}\right) d\boldsymbol{r}_1 \quad (17)$$

which means that $W_{rad}^{e}(t) \neq W_{rad}^{m}(t)$. This is not correct in free space because we have $E(r,t) \approx \eta_0 H(r,t)$ for far field in free space, from which we can verify that in free space the electric radiative energy has to be equal to the magnetic radiative energy. Therefore, either $W_{\rho}(t)$ or $W_{J}(t)$, or even both of them, cannot be treated as reactive energy.

Integrating (9) over a finite domain $V_a \supset V_s$ and rearranging the terms gives

$$\int_{V_a} \left(\frac{1}{2}\rho\phi\right) d\boldsymbol{r}_1 = \int_{V_a} \left(\frac{1}{2}\boldsymbol{D} \cdot \boldsymbol{E} + \frac{1}{2}\boldsymbol{D} \cdot \frac{\partial \boldsymbol{A}}{\partial t}\right) d\boldsymbol{r}_1 + \oint_{S_a} \frac{1}{2}\phi \boldsymbol{D} \cdot \hat{\boldsymbol{n}} dS \quad (18)$$

where S_a is the surface enclosing V_a with outward normal unit $\hat{\mathbf{n}}$. In order to investigate the property of $W_{\rho}(t)$, we assume $T \to +\infty$ so that the fields can spread over the whole space. Let $r \to \infty$, then we have $V_a \to V_\infty$ and $S_a \to S_\infty$.(Note: in this case, the fields on S_a are not zero, so the surface integral is not zero. We consider its asymptotic behavior when $S_a \to S_\infty$.) Recalling that $\lim_{r\to\infty}(\mathbf{D} \cdot \hat{\mathbf{r}}) \sim O\left(\frac{1}{r^2}\right)$ and $\lim_{r\to\infty}\phi \sim O\left(\frac{1}{r}\right)$, where $\hat{\mathbf{r}}$ is the unit radial vector, the surface integral at the RHS of (18) approaches zero when $S_a \to S_\infty$. The energy at the LHS of (18), i.e., $W_{\rho}(t)$, really has the meaning of being stored in the space with no energy leaking to the infinity. Therefore, it is at least not improper to define $W_{\rho}(t)$ as the electric reactive energy.

Follow the same procedure, integrating (10) over the domain $V_a \supset V_s$ and rearranging the terms gives

$$\int_{V_a} \left(\frac{1}{2}\boldsymbol{J} \cdot \boldsymbol{A}\right) d\boldsymbol{r}_1 = \int_{V_a} \left(\frac{1}{2}\boldsymbol{B} \cdot \boldsymbol{H} - \frac{1}{2}\frac{\partial \boldsymbol{D}}{\partial t} \cdot \boldsymbol{A}\right) d\boldsymbol{r}_1 + \oint_{S_a} \left(\frac{1}{2}\boldsymbol{H} \times \boldsymbol{A}\right) \cdot \hat{\boldsymbol{n}} dS \quad (19)$$

When $T \to +\infty$, we have $\lim_{r\to\infty}(\mathbf{H} \times \mathbf{A}) \cdot \hat{\mathbf{r}} \sim O\left(\frac{1}{r^2}\right)$, the surface integral in (19) when $S_a \to S_\infty$ is usually a bounded but nonzero value. The LHS of (19), i.e., $W_{J}(t)$, which is obviously not an energy purely stored in the whole space V_∞ because a part of the energy will eventually leak into the infinity, which is related to the electromagnetic radiation. Therefore, it is not proper to define $W_{J}(t)$ as the magnetic reactive energy. This has also been verified in our previous works [35]-[37]. In the case of the Hertzian dipole, the reactive electric energy defined by $W_{\rho}(t)$ is exactly in agreement with the electric energy stored in the capacitor in its equivalent circuit model proposed by Chu [4]. However, the magnetic reactive energy calculated with $W_{J}(t)$ does not exactly equal to the magnetic energy stored in the equivalent inductor.

Therefore, we conclude that it is proper to treat $W_{\rho}(t)$ as the electric reactive energy, and let the electric radiative energy equal to the magnetic radiative energy,

$$W_{rad}^{m}(t) = W_{rad}^{e}(t) = \frac{1}{2}W_{rad}(t) = -\int_{V_\infty} \left(\frac{1}{2}\boldsymbol{D} \cdot \frac{\partial \boldsymbol{A}}{\partial t}\right) d\boldsymbol{r}_1 \quad (20)$$

Consequently, we have

$$W_{tot}^{e}(t) = W_{\rho}(t) + W_{rad}^{e}(t) \quad (21)$$

$$W_{tot}^{m}(t) = W_{J}(t) + W_{rad}^{m}(t) + \int_{V_\infty} \frac{1}{2}\frac{\partial}{\partial t}(\boldsymbol{D} \cdot \boldsymbol{A}) d\boldsymbol{r}_1 \quad (22)$$

It has been demonstrated that the last term in the RHS of (22) is corresponding to the Schott energy in the charged particle theory [39][40] by applying the Lienard-Wiechert potentials [41] to a moving charge [42][38]. We denote it as the macroscopic Schott energy,

$$W_S(t) = \int_{V_\infty} \frac{1}{2}\frac{\partial}{\partial t}(\boldsymbol{D} \cdot \boldsymbol{A}) d\boldsymbol{r}_1 \quad (23)$$

3. The Time Domain Explicit Expressions for the Energies

With the above logistical reasoning, we proposed the energy separation formulation:

$$W_{tot}(t) = W_{\rho J}(t) + W_{rad}(t) + W_S(t) \quad (24)$$

We want to verify this separation mainly by (i) checking the non-zero period of each energy to reveal their property in time domain;(ii) numerical verifying it with Hertzian dipole; (iii) demonstrating the consistency of the time formulation and frequency domain formulation. So we derive the explicit expressions in this section, and check the Hertzian dipole in the next section.

For a pulse radiator in $[0,T]$, the scalar potential $\phi(\mathbf{r},t)$ and the vector potential $\mathbf{A}(\mathbf{r},t)$ evaluated at the observation point $\mathbf{r}$ and the time t are defined in their usual way,

$$\phi(\boldsymbol{r},t)=\int_{V_S}\frac{\rho(r_1,t\prime)}{4\pi\varepsilon_0 R_1}d\boldsymbol{r}_1=\frac{\rho}{4\pi\varepsilon_0}\int_{V_S}\frac{\rho(r_1)}{R_1}*\delta\left(t-\frac{R_1}{c}\right)d\boldsymbol{r}_1 \quad (25)$$

$$\boldsymbol{A}(\boldsymbol{r},t)=\mu_0\int_{V_S}\frac{J(r_1,t\prime)}{4\pi R_1}d\boldsymbol{r}_1=\frac{\mu_0}{4\pi}\int_{R_S}\frac{J(r_1)}{R}*\delta\left(t-\frac{R_1}{c}\right)d\boldsymbol{r}_1 \quad (26)$$

In the above equations, $t'=t-R_1/c$ is the retarded time, and c is the light velocity in vacuum and $R_1=|\mathbf{r}-\mathbf{r}_1|$ is the distance between the two positions.

In order to reveal the property of the macroscopic Schott energy, we are to derive its explicit expression from the vector potential and the electric flux density,

$$\boldsymbol{D}(\boldsymbol{r},t)=-\varepsilon_0\nabla\phi(\boldsymbol{r},t)-\varepsilon_0\frac{\partial}{\partial t}\boldsymbol{A}(\boldsymbol{r},t)=-\int_{V_S}\nabla\frac{\rho(\boldsymbol{r}_1,t')}{4\pi R_1}d\boldsymbol{r}_1-\mu_0\varepsilon_0\int_{V_S}\frac{\partial}{\partial t}\frac{\boldsymbol{J}(\boldsymbol{r}_1,t')}{4\pi R_1}d\boldsymbol{r}_1$$

$$=-\int_{V_S}\int_{-\infty}^{\infty}\rho(\boldsymbol{r}_1,t_1)\nabla G\left(t-t_1-\frac{R_1}{c}\right)dt_1\,d\boldsymbol{r}_1-\frac{1}{c^2}\int_{V_S}\int_{-\infty}^{\infty}\boldsymbol{J}(\boldsymbol{r}_1,t_1)\dot{G}\left(t-t_1-\frac{R_1}{c}\right)dt_1\,d\boldsymbol{r}_1 \quad (27)$$

where the superscript "$\cdot$" means derivative with respect to time. The time domain Green's function can be expressed with the Dirac delta function,

$$\boldsymbol{G_1}\left(\boldsymbol{r},\boldsymbol{r_1};\boldsymbol{t}-\frac{\boldsymbol{R_1}}{\boldsymbol{c}}\right)=\frac{\boldsymbol{\delta}\left(\boldsymbol{t}-\frac{\boldsymbol{R_1}}{\boldsymbol{c}}\right)}{\boldsymbol{4\pi R_1}} \quad (28)$$

Substituting (26) and (27) into (23) yields

$$\boldsymbol{W_S(t)}=\int_{V_\infty}\frac{\boldsymbol{1}}{\boldsymbol{2}}\frac{\boldsymbol{\partial}}{\boldsymbol{\partial t}}(\boldsymbol{D}\cdot\boldsymbol{A})\boldsymbol{dr}$$

$$=-\boldsymbol{\mu_0}\int_{V_\infty}\int_{V_S}\int_{V_S}\left\{\left[\int_{-\infty}^{\infty}\boldsymbol{\rho(r_1,t_1)\nabla G_1dt_1}+\boldsymbol{c^{-2}}\int_{-\infty}^{\infty}\boldsymbol{J(r_1,t_1)\dot{G}_1dt_1}\right]\cdot\int_{-\infty}^{\infty}\boldsymbol{J(r_2,t_2)G_2dt_2}\right\}\boldsymbol{dr_1dr_2\,dr} \quad (29)$$

where $G_{1,2}=G\left(t-t_{1,2}-\frac{R_{1,2}}{c}\right)$ and $R_{1,2}=\left|\mathbf{r}-\mathbf{r}_{1,2}\right|$. Note that $\rho(\mathbf{r}_1,t_1)$, $\mathbf{J}(\mathbf{r}_1,t_1)$ and $\rho(\mathbf{r}_2,t_2)$, $\mathbf{J}(\mathbf{r}_2,t_2)$ stand for the sources at $(\mathbf{r}_1,t_1)$ and $(\mathbf{r}_2,t_2)$, respectively. They are the same function related to the same radiator. Now we take the first term of $W_S(t)$ as an example to show the derivation. Rearranging the integration order gives:

$$\boldsymbol{W_S^{\rho}(t)}=-\boldsymbol{\mu_0}\frac{\boldsymbol{1}}{\boldsymbol{2}}\frac{\boldsymbol{\partial}}{\boldsymbol{\partial t}}\int_{V_S}\int_{V_S}\int_{-\infty}^{\infty}\int_{-\infty}^{\infty}\boldsymbol{J(r_1,t_1)\rho(r_2,t_2)}\cdot\int_{V_\infty}\boldsymbol{G_1\nabla G_2drdt_2\,dt_1dr_2dr_1} \quad (30)$$

Making use of the identity $G_1\nabla G_2=\nabla(G_1G_2)-\nabla G_1G_2$ and $\mathbf{J}_1\cdot\nabla G_1=-\mathbf{J}_1\cdot\nabla_1G_1=G_1\nabla_1\cdot\mathbf{J}_1-\nabla_1\cdot(\mathbf{J}_1G_1)$, and noticing that the surface integrals at S_∞ are zeros, we get

$$\boldsymbol{W_S^{\rho}(t)}=-\boldsymbol{\mu_0}\frac{\boldsymbol{\partial}}{\boldsymbol{\partial t}}\int_{V_S}\int_{V_S}\int_{-\infty}^{\infty}\int_{-\infty}^{\infty}\boldsymbol{\nabla_1\cdot J(r_1,t_1)\rho(r_2,t_2)}\int_{V_\infty}\boldsymbol{G_1G_2drdt_2\,dt_1dr_2dr_1} \quad (31)$$

It is required to evaluate the following integral associated with two source point $\mathbf{r}_1$ and $\mathbf{r}_2$,

$$\boldsymbol{I}=\int_{V_\infty}\boldsymbol{G}\left(\boldsymbol{\tau_1}-\frac{\boldsymbol{R_1}}{\boldsymbol{c}}\right)\boldsymbol{G}\left(\boldsymbol{\tau_2}-\frac{\boldsymbol{R_2}}{\boldsymbol{c}}\right)\boldsymbol{dr}=\frac{\boldsymbol{c^2}}{\boldsymbol{16\pi^2}}\int_{V_\infty}\frac{\boldsymbol{1}}{\boldsymbol{R_1R_2}}\boldsymbol{\delta(c\tau_1-R_1)\delta(c\tau_2-R_2)dr} \quad (32)$$

where $\tau_{1,2}=t-t_{1,2}$, $R_{1,2}=\left|\mathbf{r}-\mathbf{r}_{1,2}\right|$. The value of the integral has been given in the equation (32) in [30]. Here we provide an alternative rigorous proof. In the spherical coordinates, choose $\mathbf{r}_1$ as the origin and put $\mathbf{r}_2$ on +z axis, as shown in Fig.2(a). Therefore, we can write $\mathbf{r}_2=r_{21}\hat{\mathbf{z}}$, $R_1=|\mathbf{r}|=r$, and $R_2=|\mathbf{r}-\mathbf{r}_2|=\sqrt{r^2-2rr_{21}\cos\theta+r_{21}^2}$. Since the integrand is symmetric, we have

$$\boldsymbol{I}=\frac{\boldsymbol{c^2}}{\boldsymbol{8\pi}}\int_{\boldsymbol{0}}^{\pi}\int_{\boldsymbol{0}}^{\infty}\frac{\boldsymbol{1}}{\boldsymbol{rR_2}}\boldsymbol{\delta(c\tau_1-r)\delta(c\tau_2-R_2)r^2\sin\theta\,drd\theta}=\frac{\boldsymbol{c^2}}{\boldsymbol{8\pi}}\int_{-\boldsymbol{1}}^{\boldsymbol{1}}\frac{\boldsymbol{c\tau_1}}{\boldsymbol{R_2}}\boldsymbol{\delta(c\tau_2-R_2)d\cos\theta}$$

$$=-\frac{\boldsymbol{c^2}}{\boldsymbol{8\pi}}\int_{|\boldsymbol{c\tau_1-r_{21}}|}^{\boldsymbol{c\tau_1+r_{21}}}\frac{\boldsymbol{c\tau_1}}{\boldsymbol{R_2}}\boldsymbol{\delta(c\tau_2-R_2)}\left(-\frac{\boldsymbol{R_2}}{\boldsymbol{c\tau_1r_{21}}}\right)\boldsymbol{dR_2}=\frac{\boldsymbol{c^2}}{\boldsymbol{8\pi r_{21}}} \quad (33)$$

where $dR_2=-(c\tau_1r_{21}/R_2)d\cos\theta$ is used. Apparently, the integration is nonzero only when $c\tau_2$ falls into the range of the integration, i.e., $|c\tau_1-r_{21}|\le c\tau_2\le c\tau_1+r_{21}$, and satisfy conditions of $0\le\tau_{1,2}\le t$ and $R_1+R_2\ge r_{21}$. Therefore, we have

$$\begin{cases} -\tau_2 \le \tau_1 - \frac{r_{21}}{c} \le \tau_2 \\ \tau_2 \le \tau_1 + \frac{r_{21}}{c} \\ \tau_{1,2} \le t \\ c(2t - \tau_1 - \tau_2) \ge \frac{r_{21}}{c} \end{cases} \tag{34}$$

which leads to

$$\begin{cases} \frac{r_{21}}{c} - \tau_2 \le \tau_1 \le \tau_2 + \frac{r_{21}}{c}, & \tau_2 \le \frac{r_{21}}{c} \\ \tau_2 - \frac{r_{21}}{c} \le \tau_1 \le \tau_2 + \frac{r_{21}}{c}, & \frac{r_{21}}{c} \le \tau_2 \le t - \frac{r_{21}}{c} \\ \tau_2 - \frac{r_{21}}{c} \le \tau_1 \le 2t - \tau_2 - \frac{r_{21}}{c}, & t - \frac{r_{21}}{c} \le \tau_2 \le t \end{cases} \tag{35}$$

This is the integration range of (τ_1, τ_2) for nonzero I. It is the shadowed rectangular area shown in Fig. 2(b). which is similar to that in [30] (Fig.2 in [30]). (35) is the same as eq. (33) in [30]. If the sources are zero for $t < 0$, the integration area shown in Fig. 2(b) is rigorous. Note that the integration region in [30] can get correct result if we substitute the condition that the sources are zero when $t < 0$ in the derivation.

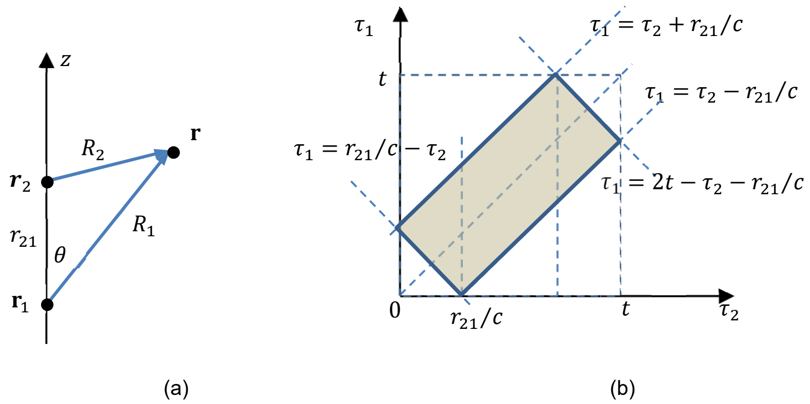

Fig. 2. Evaluating the integral I. (a) The coordinate system. (b) Integration region.

Performing the double integration ($\int\int dt_1 dt_2$) on the region shown in Fig. 2(b), and dividing the inner integration into three sub-regions gives

$$W_S^{\rho}(t) = -\frac{\mu_0 c^2}{16\pi}\frac{\partial}{\partial t}\int_{V_s}\int_{V_s}\frac{1}{r_{21}}\left\{\begin{aligned} &\int_0^{\frac{r_{21}}{c}} \rho\left(r_2, t_1 + \frac{r_{21}}{c}\right)\rho(r_1, t_1)dt_1 \\ &+\int_{\frac{r_{21}}{c}}^{t-\frac{r_{21}}{c}} \left[\rho\left(r_2, t_1 + \frac{r_{21}}{c}\right) - \rho\left(r_2, t_1 - \frac{r_{21}}{c}\right)\right]\rho(r_1, t_1)dt_1 \\ &+\int_{t-\frac{r_{21}}{c}}^{t}\left[\rho\left(r_2, 2t - t_1 - \frac{r_{21}}{c}\right) - \rho\left(r_2, t_1 - \frac{r_{21}}{c}\right)\right]\rho(r_1, t_1)dt_1 \end{aligned}\right\} dr_2 dr_1$$

$$= -\frac{\mu_0 c^2}{8\pi}\int_{V_s}\int_{V_s}\int_{t-\frac{r_{21}}{c}}^{t}\left[\frac{1}{r_{21}}\rho(r_1, t_1)\dot{\rho}\left(r_2, 2t - t_1 - \frac{r_{21}}{c}\right)\right] dt_1\, dr_2 dr_1 \tag{36}$$

Replacing t_1 by τ and evaluating the second term in a similar way we can get (37),

$$W_S(t) = -\frac{1}{8\pi\varepsilon_0}\int_{V_s}\int_{V_s}\frac{1}{r_{21}}\int_{t-\frac{r_{21}}{c}}^{t}\left[\rho(r_1,\tau)\dot{\rho}\left(r_2, 2t-\tau-\frac{r_{21}}{c}\right) + c^{-2}\dot{J}\left(r_1, 2t-\tau-\frac{r_{21}}{c}\right)\cdot J(r_2,\tau)\right] d\tau dr_2 dr_1 \tag{37}$$

where $r_{21} = |\mathbf{r}_2 - \mathbf{r}_1|$. The nonzero range can be determined by noting that the sources exist within $[0, T]$ and at least one of the source terms is zero for $t \ge T + 0.5t_{max}$, where $t_{max} = r_{21,max}/c$ is the largest travelling time between two source points. This means that after the sources have disappeared, although $\partial(\mathbf{D}\cdot\mathbf{A})/\partial t$ is not zero everywhere in the space, its volume integral over the whole space, i.e., $W_S(t)$, soon becomes zero.

Using the same technique, the principal radiative energy can be evaluated with the integration over the source region,

$$W_{rad}^{pri}(t) = \frac{1}{8\pi\varepsilon_0}\int_{V_s}\int_{V_s}\frac{1}{r_{21}}\int_{\frac{r_{21}}{c}}^{t}\left\{\begin{aligned} &\left[\dot{\rho}(r_1,\tau)\rho\left(r_2,\tau-\frac{r_{21}}{c}\right) - \dot{\rho}\left(r_1,\tau-\frac{r_{21}}{c}\right)\rho(r_2,\tau)\right] \\ &+c^{-2}\left[J(r_1,\tau)\dot{J}\left(r_2,\tau-\frac{r_{21}}{c}\right) - J\left(r_1,\tau-\frac{r_{21}}{c}\right)\cdot\dot{J}(r_2,\tau)\right]\end{aligned}\right\} d\tau dr_2 dr_1 \tag{38}$$

It can be checked that for a pulse source over $[0,T]$, $W_{rad}^{pri}(t) = W_{rad}^{pri}(T)$ for $t \geq T$. However, the total radiative energy continues to vary in a small time period $[T, T + 0.5t_{max}]$ due to the effect of $W_S(t)$.

Similarly, the explicit expressions for the Coulomb-velocity energy are

$$\boldsymbol{W_\rho(t)} = \frac{1}{8\pi\varepsilon_0}\int_{V_s}\int_{V_s}\frac{1}{r_{21}}\boldsymbol{\rho(r_1,t)\rho(r_2,t-r_{21}/c)\,dr_1\,dr_2} \quad (39)$$

$$\boldsymbol{W_J(t)} = \frac{\mu_0}{8\pi}\int_{V_s}\int_{V_s}\frac{1}{r_{21}}\boldsymbol{J(r_1,t)\cdot J(r_2,t-r_{21}/c)\,dr_1\,dr_2} \quad (40)$$

4. Hertzian Dipole

The moment of the dipole is assumed to be $ql\cos\omega t$, the scalar potential and the vector potential of which can be readily derived from the Hertzian potential $\Pi = (ql/4\pi r)\cos(\omega t - kr)$ [36][43],

$$\boldsymbol{A} = -\frac{\omega\mu_0 ql}{4\pi r}\boldsymbol{\sin(\omega t - kr)\left(\hat{r}\cos\theta - \hat{\theta}\sin\theta\right)} \quad (41)$$

$$\boldsymbol{\varphi} = \frac{\omega^2\mu_0 ql}{4\pi}\boldsymbol{\cos\theta\left[\frac{1}{k^2r^2}\cos(\omega t - kr) - \frac{1}{kr}\sin(\omega t - kr)\right]} \quad (42)$$

from which the fields are found to be

$$\boldsymbol{E} = \frac{k^2 ql}{4\pi\varepsilon_0 r}\boldsymbol{\left\{\hat{r}2\cos\theta\frac{1}{kr}\left[\frac{1}{kr}\cos(\omega t - kr) - \sin(\omega t - kr)\right] + \hat{\theta}\sin\theta\left[\left(\frac{1}{k^2r^2} - 1\right)\cos(\omega t - kr) - \frac{1}{kr}\sin(\omega t - kr)\right]\right\}} \quad (43)$$

$$\boldsymbol{H} = -\frac{\omega kql}{4\pi r}\boldsymbol{\sin\theta\left[\frac{1}{kr}\sin(\omega t - kr) + \cos(\omega t - kr)\right]\hat{\varphi}} \quad (44)$$

As is known, the Hertzian dipole is a point source and its total reactive energy is infinite. A common strategy is to evaluate the energies with integrands containing fields and potentials in the whole space excluding a small sphere with radius a. The results are listed below,

$$\boldsymbol{W_{react}^e(t)} = \int_{V_\infty - V_a}\boldsymbol{\left(\frac{1}{2}D\cdot E + \frac{1}{2}D\cdot\frac{\partial A}{\partial t}\right)dr_1} = \boldsymbol{\alpha_0\left[\frac{1}{k^3a^3} + \frac{1}{ka} + \left(\frac{1}{k^3a^3} - \frac{1}{ka}\right)\cos 2\,(\omega t - ka) - \frac{2}{k^2a^2}\sin 2\,(\omega t - ka)\right]} \quad (45)$$

$$\boldsymbol{W_{react}^m(t)} = \int_{V_\infty - V_a}\boldsymbol{\left(\frac{1}{2}B\cdot H + \frac{1}{2}D\cdot\frac{\partial A}{\partial t}\right)dr_1} = \frac{2\alpha_0}{ka}\boldsymbol{\sin^2(\omega t - ka)} \quad (46)$$

where $\alpha_0 = (\omega ql)^2\mu_0 k/(24\pi)$. The principal radiative power evaluated at a spherical observation surface is

$$\boldsymbol{P_{rad}^{pri}(t)} = \oint_{S_a}\boldsymbol{S_{Srad}\cdot\hat{n}dS = 2\omega\alpha_0} \quad (47)$$

It is a constant value independent of the radius of the sphere, clearly indicating that the total principal radiative power associated with $W_{rad}^{pri}(t)$ passing through any concentric spherical surface is identical.

The Poynting power flux on the spherical surface S_a is calculated to be

$$\boldsymbol{P_{pv}(t)} = \oint_{S_a}\boldsymbol{S\cdot\hat{n}dS = 2\omega\alpha_0[1 + \cos 2\,(\omega t - ka)] + 2\omega\alpha_0\left[\left(\frac{2}{ka} - \frac{1}{k^3a^3}\right)\sin 2\,(\omega t - ka) - \frac{2}{k^2a^2}\cos 2\,(\omega t - ka)\right]} \quad (48)$$

which decreases with the radius of the surface due to the effect of the reactive energy. As expected, the time average of $P_{pv}(t)$ equals to that of $P_{rad}^{pri}(t)$.

Since the Hertzian dipole is a point source, its fields propagate radially and cross all concentric spherical observation surfaces with light velocity. Therefore, the radiative energy per unit time near the spherical surface S_a can be considered as the real radiative power crossing S_a,

$$\boldsymbol{P_{rad}^{real}(t)dt} = \int_S\int_a^{a+cdt}\boldsymbol{\left(-D\cdot\frac{\partial A}{\partial t}\right)drdS = cdt}\int_{S_a}\boldsymbol{\left(-D\cdot\frac{\partial A}{\partial t}\right)dS} \quad (49)$$

from which the real radiative power is found exactly to be

$$\boldsymbol{P_{rad}^{real}(t) = 2\omega\alpha_0[1 + \cos 2\,(\omega t - ka)]} \quad (50)$$

the amplitude of which is not dependent on the radius of the observation surface. It is readily to recognize from (48) that it is the first term in the Poynting power flux $P_{pv}(t)$. The other terms of $P_{pv}(t)$ in (48) compose the pseudo power flow, which decreases with the distance to the dipole.

$$\boldsymbol{P_{rad}^{pseudo}(t) = 2\omega\alpha_0\left[\left(\frac{2}{ka} - \frac{1}{k^3a^3}\right)\sin 2\,(\omega t - ka) - \frac{2}{k^2a^2}\cos 2\,(\omega t - ka)\right]} \quad (51)$$

The time averaged energies are listed below for readers' reference,

$$\begin{cases}(\boldsymbol{W_m})_{av} = \boldsymbol{\alpha_0}\left(\frac{1}{ka}\right) \\ (\boldsymbol{W_e})_{av} = \boldsymbol{\alpha_0}\left(\frac{1}{k^3a^3}+\frac{1}{ka}\right)\end{cases} \tag{52}$$

The Q factor of the dipole is then calculated to be

$$\boldsymbol{Q} = \frac{2\omega(W_e)_{av}}{(P_{rad})_{av}} = \frac{1}{k^3a^3}+\frac{1}{ka} \tag{53}$$

which is exactly in agreement with the result shown in [3].

The well-established equivalent circuit model proposed by Chu [4] for Hertzian dipole is shown in Fig.3(b). Assume that the current in the radiation resistor at the interface of $r = a$ is $i_R = I_0\cos(\omega t - ka)$. The energies stored in the capacitor and the inductor can be derived to be

$$\begin{cases}\boldsymbol{W_C(t)} = \frac{I_0^2}{4\omega}\left[\frac{1}{ka}+\frac{1}{k^3a^3}+\left(\frac{1}{k^3a^3}-\frac{1}{ka}\right)\boldsymbol{\cos 2\,(\omega t - ka)} - \frac{2}{(ka)^2}\boldsymbol{\sin 2\,(\omega t - ka)}\right] \\ \boldsymbol{W_L(t)} = \frac{I_0^2}{2\omega}\left(\frac{1}{ka}\boldsymbol{\sin^2(\omega t - ka)}\right)\end{cases} \tag{54}$$

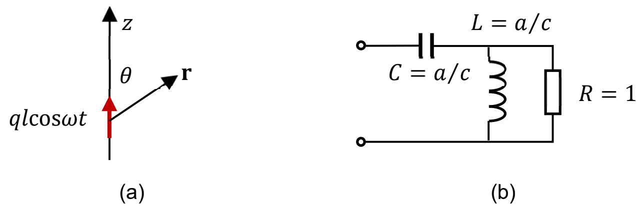

Fig. 3. Hertzian dipole. (a) Coordinate system. (b) Equivalent circuit model.

If we choose $I_0^2 = 4\omega\alpha_0$, it can be readily verified that $W_C(t) = W_e(t)$ and $W_L(t) = W_m(t)$.

The integration regions for $W_{rad}(t)$, $W_{rad}^{pri}(t)$ and $W_S(t)$ are all modified in a similar way. They are found to be

$$\boldsymbol{W_{rad}(t)} = -\int_{V_\infty - V_a}\boldsymbol{D}\cdot\frac{\partial \boldsymbol{A}}{\partial t}\boldsymbol{dV} = \boldsymbol{2k\alpha_0}\lim_{r\to\infty}(\boldsymbol{r}-\boldsymbol{a}) + \boldsymbol{\alpha_0}\left[\boldsymbol{\sin 2\,(\omega t - ka)} - \lim_{r\to\infty}\boldsymbol{\sin 2\,(\omega t - kr)}\right] \tag{55}$$

$$\boldsymbol{W_{rad}^{pri}(t)} = \int_{V_\infty - V_a}\frac{1}{2}\left(\frac{\partial \boldsymbol{D}}{\partial t}\cdot\boldsymbol{A} - \boldsymbol{D}\cdot\frac{\partial \boldsymbol{A}}{\partial t}\right)\boldsymbol{dV} = \boldsymbol{2\alpha_0 k}\lim_{r\to\infty}(\boldsymbol{r}-\boldsymbol{a}) \tag{56}$$

$$\boldsymbol{W_S(t)} = \int_{V_\infty - V_a}\frac{\partial}{\partial t}\left(\frac{1}{2}\boldsymbol{D}\cdot\boldsymbol{A}\right)\boldsymbol{dV} = -\boldsymbol{\alpha_0}\left[\boldsymbol{\sin 2\,(\omega t - ka)} - \lim_{r\to\infty}\boldsymbol{\sin 2\,(\omega t - kr)}\right] \tag{57}$$

With the wave travels to infinity, the principal radiative energy $W_{rad}^{pri}(t)$ monotonically increases with the radius, revealing that the radiative rate is always positive. The macroscopic Schott energy $W_S(t)$ oscillates in the propagation with a zero average value. Its amplitude remains constant in this case.

We want to remind readers that no other numerical methods can provide such an accurate verification of the energy relationship in Hertzian dipole.

5. Explanation for Negative Energies

In the article, the surface current on a ring described by $\mathbf{J}_s(\mathbf{r},t) = I(t)\hat{\varphi}$ [A/m] is a solenoidal current with zero charge density, $I(t) = e^{-\gamma^2}\sin\omega t$ is a modulated Gaussian pulse. The reactive energy includes the contribution from the current alone, i.e., W_J. It oscillates with the source and admits negative values periodically, as shown in Fig. 4. Negative W_J is acceptable because the reactive energy is dependent on the potentials, which are values relative to their reference zero points. When the current varies and changes its direction periodically, the retarded vector potential in the source region lags behind and may point in direction opposite to that of the current, causing negative values of W_J. A source itself can radiate energy. It can also interact with fields radiated by other sources and absorb part of the energies carried by the fields. Consider a part of the loop current. On the one hand, it will radiate energy to the space, which will propagate to the other part of the loop current and interact with them; on the other hand, it will interact with fields radiated by the other part of the loop current some time earlier and absorb part of the energy of the fields. In the article, it is considered that the source absorbs more energy than that it radiates when its W_J is negative.

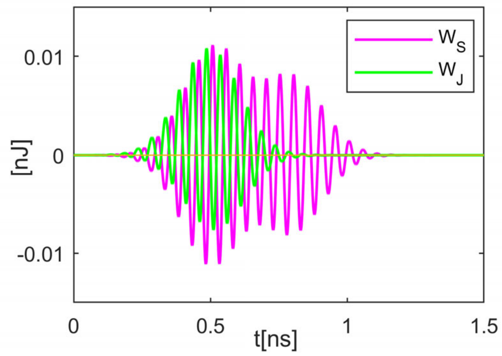

Fig.4. The energy of the loop current evaluated in the source region.

Although we prefer the explanation that the negative energy is caused by energy absorption, we also give here another possible explanation. Consider a loop current with radius b and current $I(t)\hat{\varphi}$, as shown in Fig. 5(a)., the magnetic flux generated by the loop current is

$$\boldsymbol{\Phi}(\boldsymbol{t}) = \int_S \boldsymbol{B}(\boldsymbol{r},\boldsymbol{t}) \cdot \hat{\boldsymbol{n}} \boldsymbol{dS} = \oint_C \boldsymbol{A}(\boldsymbol{r},\boldsymbol{t}) \cdot \boldsymbol{b}\hat{\boldsymbol{\varphi}}_1 \boldsymbol{d\varphi}_1 = \frac{\mu_0 b^2}{4\pi} \oint_C \oint_C \frac{1}{r_{21}} \boldsymbol{I}\left(\boldsymbol{t} - \frac{r_{21}}{c}\right)(\hat{\boldsymbol{\varphi}}_1 \cdot \hat{\boldsymbol{\varphi}}_2) \boldsymbol{d\varphi}_2 \boldsymbol{d\varphi}_1 \quad (58)$$

where $r_{21} = 2b\sin\big(0.5(\varphi_1 - \varphi_2)\big)$ is the distance between two points on the loop. In circuit theory, the associated inductance associated with the loop current is defined as $L = \Phi/I$, and the energy stored in the inductor is expressed by

$$\boldsymbol{W}_L = \frac{1}{2}\boldsymbol{L}\boldsymbol{I}^2 \quad (59)$$

At low frequencies, the magnetic flux is always positive, as most of the magnetic fields inside the loop can catch up with the change of the current and pass through the curvature S in the same direction, as shown in Fig. 5(a). However, at high frequencies, because of the retardation of the fields, some of the magnetic field inside the loop may cross the curvature S in opposite direction, as shown in Fig.5(b). The total magnetic flux through the curvature S may become negative if we calculate it with (58), therefore, we will have a negative inductance. According to (59), the magnetic energy becomes negative.

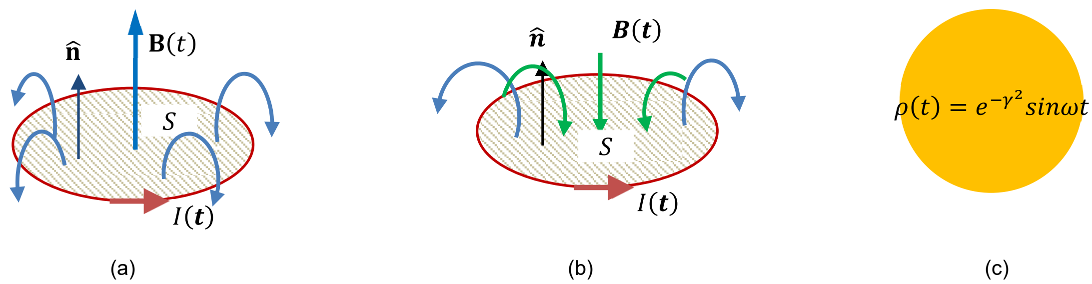

Fig. 5. Loop current and disk charge sources. (a) Magnetic flux of a loop current corresponding to positive inductance at low frequencies. (b) Corresponding to a negative inductance at high frequencies. (c) Charge density on a disk plate.

For readers' reference, we have also confirmed that a harmonic charge density, e.g., $\rho(t) = e^{-\gamma^2}\sin\omega t$ in Fig. 5(c), uniformly distributed on a disk plate sometimes may have negative Coulomb energy $W_\rho(t)$.

6. Numerical Technique in MOT

For a PEC antenna (we consider PEC plate with zero thickness), we calculate the energies in two steps. Firstly, we calculate the surface currents by solving the surface electric field integral equation (EFIE) with marching-on in time scheme (MOT) [44][45]. Secondly, based on equivalence principle, we assume that the surface currents are in free space, and calculate the associated energies with the expressions we have proposed.

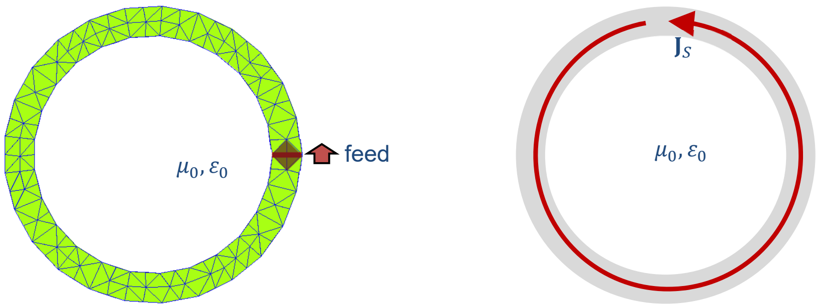

(a) (b)

Fig. 6. Antenna radiation problem. (a) PEC loop antenna with Delta-gap voltage feeding, triangularly-meshed. (b) Equivalent problem with its surface currents in free space.

The surface current on the PEC radiator is subject to the time domain electric field integral equation (TD-EFIE):

$$\left[\frac{\partial \boldsymbol{A}(\boldsymbol{r},t)}{\partial t} + \nabla \boldsymbol{\phi}(\boldsymbol{r},\boldsymbol{t})\right]_{tan} = \boldsymbol{E}^{feed}(\boldsymbol{r},\boldsymbol{t})\Big|_{tan} \tag{60}$$

We can expand the surface current with N RWG bases $\mathbf{f}_n(\mathbf{r})$

$$\boldsymbol{J}_s(\boldsymbol{r},\boldsymbol{t}) = \sum_{n=1}^{N} \boldsymbol{I}_n(\boldsymbol{t}) \boldsymbol{f}_n(\boldsymbol{r}) \tag{61}$$

and the surface charge density with

$$\boldsymbol{\rho}_s(\boldsymbol{r},\boldsymbol{t}) = -\sum_{n=1}^{N} \int_{-\infty}^{t} \boldsymbol{I}_n(\xi) d\xi \nabla \cdot \boldsymbol{f}_n(\boldsymbol{r}) = \sum_{n=1}^{N} \nabla \cdot \boldsymbol{f}_n(\boldsymbol{r}) \boldsymbol{q}_n(\boldsymbol{t}) \tag{62}$$

As shown in Fig. 7., The RWG basis function is defined as [46]

$$\boldsymbol{f}_n(\boldsymbol{r}) = \begin{cases} \boldsymbol{C}_n^{+}(\boldsymbol{r} - \boldsymbol{r}_n^{+}), \boldsymbol{r} \in \boldsymbol{T}_n^{+} \\ -\boldsymbol{C}_n^{-}(\boldsymbol{r} - \boldsymbol{r}_n^{-}), \boldsymbol{r} \in \boldsymbol{T}_n^{-} \end{cases}, \boldsymbol{C}_n^{\pm} = \frac{l_n}{2A_n^{\pm}}, \nabla_s \cdot \boldsymbol{f}_n(\boldsymbol{r}) = 2\boldsymbol{C}_n \tag{63}$$

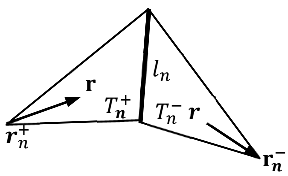

Fig. 7. RWG basis function

Rewrite the potentials as convolutions in time,

$$\boldsymbol{A}(\boldsymbol{r},\boldsymbol{t}) = \frac{\mu_0}{4\pi} \int_S \frac{J_s(r_1)}{R_1} * \boldsymbol{\delta}\left(\boldsymbol{t} - \frac{R_1}{c}\right) \boldsymbol{dr}_1, \quad \boldsymbol{\phi}(\boldsymbol{r},\boldsymbol{t}) = \frac{1}{4\pi\varepsilon_0} \int_S \frac{\rho_s(r_1)}{R_1} * \boldsymbol{\delta}\left(\boldsymbol{t} - \frac{R_1}{c}\right) \boldsymbol{dr}_1 \tag{64}$$

Note that

$$\nabla \frac{\delta\left(t - \frac{R_1}{c}\right)}{R_1} = \left(-\frac{\delta\left(t - \frac{R_1}{c}\right)}{R_1^2} - \frac{\dot{\delta}\left(t - \frac{R_1}{c}\right)}{cR_1}\right) \widehat{\boldsymbol{a}}_R \tag{65}$$

$$\dot{\boldsymbol{A}}(\boldsymbol{r},\boldsymbol{t}) = \sum_{n=1}^{N_A} \dot{\boldsymbol{I}}_n(\boldsymbol{t}) * \frac{\mu_0}{4\pi} \int_{S_n} \boldsymbol{f}_n(\boldsymbol{r}_1) \frac{\delta\left(t - \frac{R_1}{c}\right)}{R_1} \boldsymbol{dr}_1 \tag{66}$$

Then the electric field can then be expressed by

$$\boldsymbol{E}(\boldsymbol{r},\boldsymbol{t}) = \sum_{n=1}^{N} \boldsymbol{q}_n(\boldsymbol{t}) * \frac{\boldsymbol{C}_n}{2\pi\varepsilon_0} \frac{1}{c^2 t^2} [(\boldsymbol{r} - \boldsymbol{r}_o)\boldsymbol{\Gamma}_n(\boldsymbol{r},\boldsymbol{t}) - \boldsymbol{\Gamma}_n(\boldsymbol{r},\boldsymbol{t})]$$
$$+ \sum_{n=1}^{N} \dot{\boldsymbol{q}}_n(\boldsymbol{t}) * \frac{C_n}{2\pi\varepsilon_0} \frac{1}{c^2 t} [(\boldsymbol{r} - \boldsymbol{r}_o)\boldsymbol{\Gamma}_n(\boldsymbol{r},\boldsymbol{t}) - \boldsymbol{\Gamma}_n(\boldsymbol{r},\boldsymbol{t})] + \sum_{n=1}^{N} \dot{\boldsymbol{I}}_n(\boldsymbol{t}) * \frac{C_n \mu_0}{4\pi} [(\boldsymbol{r}_n - \boldsymbol{r}_o)\boldsymbol{\Gamma}_n(\boldsymbol{r},\boldsymbol{t}) - \boldsymbol{\Gamma}_n(\boldsymbol{r},\boldsymbol{t})] \tag{67}$$

where the two functions are defined as

$$\begin{cases} \boldsymbol{\Gamma_n(r,t)} = \int_{S_n} \frac{\delta\left(t-\frac{R_1}{c}\right)}{R_1} d\boldsymbol{r_1} \\ \boldsymbol{\Gamma_n(r,t)} = \int_{S_n} (\boldsymbol{r}-\boldsymbol{r_o}) \frac{\delta\left(t-\frac{R_1}{c}\right)}{R_1} d\boldsymbol{r_1} \end{cases} \tag{68}$$

They can be evaluated analytically with formulae in [44]. The TD-EFIE (60) is transformed to a matrix equation,

$$\boldsymbol{Q^A(t)} * \boldsymbol{q(t)} + t\boldsymbol{Q^A(t)} * \dot{\boldsymbol{q}}(\boldsymbol{t}) + \boldsymbol{I^A(t)} * \dot{\boldsymbol{I}}(\boldsymbol{t}) = \boldsymbol{e^{in}(t)} \tag{69}$$

where $\boldsymbol{q}(t) = [q_1(t), q_2(t), \cdots, q_N(t)]^t$, $\mathbf{I}(t) = [I_1(t), I_2(t), \cdots, I_N(t)]^t$, $\mathbf{e}^{in}(t) = \left[e_1^{in}(t), e_2^{in}(t), \cdots, e_N^{in}(t)\right]^t$, the upper script "$t$" means transpose. The entries of the coefficient matrices are

$$\boldsymbol{Q^A_{mn}(t)} = -\frac{1}{4\pi\varepsilon_0}\int_{S_m} \boldsymbol{\nabla_s \cdot f_m(r)} \int_{S_n} \boldsymbol{\nabla_{1s} \cdot f_n(r_1)} \frac{\delta\left(t-\frac{R_1}{c}\right)}{R_1} d\boldsymbol{r_1}\, d\boldsymbol{r}$$

$$\boldsymbol{I^A(t)} = -\frac{\mu_0}{4\pi}\int_{S_m} \boldsymbol{f_m(r)} \cdot \int_{S_n} \boldsymbol{f_n(r_1)} \frac{\delta\left(t-\frac{R_1}{c}\right)}{R_1} d\boldsymbol{r_1}\, d\boldsymbol{r}$$

For PEC antennas with simple structures, we can sample $I_n(t)$ and $q_n(t)$ at discrete time $p\Delta t$ or expanding them with proper temporal basis functions, and solve the TD-EFIE with the marching-on in time method, i.e., calculate them step by step in time domain, we can obtain $I_n(t)$ and $q_n(t)$. If necessary, we may tune the time step or adopt other techniques to guarantee late time stability.

Using the obtained source data, the radiative energy and the macroscopic Schott energy can be approximately calculated with

$$\boldsymbol{W^{pri}_{rad}(t)} \approx \sum_{m=1}^N \sum_{n=1}^N \left[\boldsymbol{C^\rho_{mn}(t) I^\rho_{mn}} + \boldsymbol{C^J_{mn}(t) I^J_{mn}}\right] \tag{70}$$

$$\boldsymbol{W_S(t)} \approx \sum_{m=1}^N \sum_{n=1}^N \left[\boldsymbol{D^\rho_{mn}(t) I^\rho_{mn}} + \boldsymbol{D^J_{mn}(t) I^J_{mn}}\right] \tag{71}$$

where

$$\begin{cases} \boldsymbol{I^\rho_{mn}} = \frac{1}{8\pi\varepsilon_0}\int_{V_s}\int_{V_s} \boldsymbol{\nabla_s \cdot f_m(r_1) \nabla_s \cdot f_n(r_2) dr_2 dr_1} \\ \boldsymbol{I^J_{mn}} = \frac{1}{8\pi\varepsilon_0}\int_{V_s}\int_{V_s} \boldsymbol{f_m(r_1) \cdot f_n(r_2)\, dr_2 dr_1} \end{cases} \tag{72}$$

$$\begin{cases} \boldsymbol{C^\rho_{mn}(t)} = \frac{1}{r^c_{mn}}\int_{r^c_{mn}/c}^{t} [\boldsymbol{I_m(\tau_d) q_n(\tau) - I_m(\tau) q_n(\tau_d)}]\, d\boldsymbol{\tau} \\ \boldsymbol{C^J_{mn}(t)} = \frac{1}{c^2 r^c_{mn}}\int_{r^c_{mn}/c}^{t} [\boldsymbol{I_m(\tau) \dot{I}_n(\tau_d) - I_m(\tau_d) \dot{I}_n(\tau)}]\, d\boldsymbol{\tau} \end{cases} \tag{73}$$

$$\begin{cases} \boldsymbol{D^\rho_{mn}(t)} = \frac{1}{r^c_{mn}}\int_{t-r^c_{mn}/c}^{t} \boldsymbol{q_m(\tau) I_n(2t-2\tau+\tau_d)}\, d\boldsymbol{\tau} \\ \boldsymbol{D^J_{mn}(t)} = -\frac{1}{c^2 r^c_{mn}}\int_{t-r^c_{mn}/c}^{t} \boldsymbol{\dot{I}_m(2t-2\tau+\tau_d) I_n(\tau)}\, d\boldsymbol{\tau} \end{cases} \tag{74}$$

r^c_{mn} is the distance between the center of the triangles in the two bases, and $\tau_d = \tau - r^c_{mn}/c$. The symbol "$\cdot$" means temporal derivative. For $r^c_{mn} = 0$, (73) and (74) can be evaluated using the L'Hospital's rule. For example,

$$\lim_{r^c_{mn}\to 0} \boldsymbol{D^\rho_{mn}(t)} = \frac{\partial}{\partial r^c_{mn}}\int_{t-r^c_{mn}/c}^{t} \boldsymbol{q_m(\tau) I_n(2t-2\tau+\tau_d)}\, d\boldsymbol{\tau} = \frac{1}{c}[\boldsymbol{q_m(t) I_n(t)}] \tag{75}$$

Otherwise, the integrations have to be evaluated numerically with the values of $I_n(t)$ and $q_n(t)$ obtained with the MOT. Note that:

- Some of the coefficients have already been evaluated in the MOT process and can be reused. Modulated Gaussian pulse is often used for wideband analysis.
- The integration interval of the innermost integral is dependent on the distance between two points, and may be much smaller than the time step and should be handled carefully.

As has pointed previously, we only consider the situation in vacuum in this article. The issues like the effect of media and bulk metals, input property at the feeding port, will be presented in future work.

7. About Mutual Coupling

We consider that electromagnetic mutual coupling issue is basically the same issue as the electromagnetic radiation, and the energies involved are the same, as we have discussed in [37]. However, because of space limitation of the article, we do not include this part of content in the article.

REFERENCES

[1] R. E. Collin and S. Rothschild, “Evaluation of antenna Q,” IEEE Trans. Antennas Propag., vol. AP-12, no. 1, pp. 23–27, Jan. 1964.
[2] R. L. Fante, “Quality factor of general antennas,” IEEE Trans. Antennas Propag., vol. 17, no. 2, pp. 151–155, Mar. 1969.
[3] J. S. McLean, “A re-examination of the fundamental limits on the radiation Q of electrically small antennas,” IEEE Trans. Antennas Propag., vol. 44, no. 5, pp. 672–676, May 1996.
[4] L. J. Chu, “Physical limitations on omni-directional antennas,” J. Appl. Phys., vol. 19, no. 12, pp. 1163–1175, 1948.
[5] S. Ström, “T matrix for electromagnetic scattering from an arbitrary number of scatterers with continuously varying electromagnetic properties,” Phys. Rev. D, no.10, pp. 2685–2690, Oct. 1974.
[6] P. C. Waterman, “The T-matrix revisited,” J. Opt. Soc. Am. A, vol. 24, no. 8, pp.2257-2267, Aug. 2007.
[7] H. L. Thal, “New radiation Q limits for spherical wire antennas,” IEEE Trans. Antennas Propag., vol. 54, no. 10, pp. 2757–2763, Oct. 2006.
[8] A. D. Yaghjian and S. R. Best, “Impedance, bandwidth, and Q of antennas,” IEEE Trans. Antennas Propag., vol. 53, no. 4, pp. 1298–1324, Apr. 2005.
[9] W. Geyi, “A method for the evaluation of small antenna Q,” IEEE Trans. Antennas Propag., vol. 51, no. 8, pp. 2124–2129, Aug. 2003.
[10] S. Collardey, A. Sharaiha, and K. Mahdjoubi, “Evaluation of antenna radiation Q using FDTD method,” Electron. Lett., vol. 41, no. 12, pp. 675–677, Jun. 2005.
[11] A. D. Yaghjian, “Internal energy, Q-energy, Poynting’s theorem, and the stress dyadic in dispersive material,” IEEE Trans. Antennas Propag., vol. 55, no. 6, pp. 1495–1505, Jun. 2007.
[12] S. Collardey, A. Sharaiha, and K. Mahdjoubi, “Calculation of small antennas quality factor using FDTD method,” IEEE Antennas Wireless Propag. Lett., vol. 5, no. 1, pp. 191–194, Dec. 2006.
[13] A. Shlivinski and E. Heyman, “Time-domain near-field analysis of short pulse antennas—Part I: Spherical wave (multipole) expansion,” IEEE Trans. Antennas Propag., vol. 47, no. 2, pp. 271–279, Feb. 1999.
[14] ——, “Time-domain near-field analysis of short pulse antennas—Part II: Reactive energy and the antenna Q,” IEEE Trans. Antennas Propag., vol. 47, no. 2, pp. 280–286, Feb. 1999.
[15] D. R. Rhodes, “A reactance theorem,” Proc. R. Soc. London. A., vol. 353, no. 1672, pp. 1–10, Feb. 1977.
[16] G. A. E. Vandenbosch, “Reactive energies, impedance, and Q factor of radiating structures,” IEEE Trans. Antennas Propag., vol. 58, no. 4, pp. 1112–1127, Apr. 2010.
[17] M. Gustafsson and B. L. G. Jonsson, “Stored electromagnetic energy and antenna Q,” Prog. Electromagn. Res., vol. 150, pp. 13–27, 2015.
[18] M. Capek, P. Hazdra, and J. Eichler, “A method for the evaluation of radiation Q based on modal approach,” IEEE Trans. Antennas Propag., vol. 60, no. 10, pp. 4556–4567, Oct. 2012.
[19] P. Hazdra, M. Capek, and J. Eichler, “Comments to ‘reactive energies, impedance, and Q factor of radiating structures’ by G. Vandenbosch,” IEEE Trans. Antennas Propag., vol. 61, no. 12, pp. 6266–6267, Dec. 2013.
[20] W. Geyi, “Stored energies and radiation Q,” IEEE Trans. Antennas Propag., vol. 63, no. 2, pp. 636–645, Feb. 2015.
[21] S. M. Mikki and Y. M. M. Antar, “A new technique for the analysis of energy coupling and exchange in general antenna systems,” IEEE Trans. Antennas Propag., vol. 63, no. 12, pp. 5536–5547, Dec. 2015.
[22] K. Schab et al., “Energy stored by radiating systems,” IEEE Access, vol. 6, pp. 10553–10568, 2018.
[23] S. Mikki, D. Sarkar, and Y. M. M. Antar, “Beyond antenna Q: On reactive energy and the need for a spatio-temporal dynamical paradigm,” in Proc. 13th Eur. Conf. Antennas Propag. (EuCAP), Apr. 2019, pp. 1–4.
[24] G. A. E. Vandenbosch, “Simple procedure to derive lower bounds for radiation Q of electrically small devices of arbitrary topology,” IEEE Trans. Antennas Propag., vol. 59, no. 6, pp. 2217–2225, Jun. 2011.
[25] M. Cismasu and M. Gustafsson, “Antenna bandwidth optimization with single frequency simulation,” IEEE Trans. Antennas Propag., vol. 62, no. 3, pp. 1304–1311, Mar. 2014.
[26] M. Gustafsson and S. Nordebo, “Bandwidth, Q factor, and resonance models of antennas,” Prog. Electromagn. Res., vol. 62, pp. 1–20, 2006.
[27] M. Capek, L. Jelinek, P. Hazdra, and J. Eichler, “The measurable Q factor and observable energies of radiating structures,” IEEE Trans. Antennas Propag., vol. 62, no. 1, pp. 311–318, Jan. 2014.
[28] M. Gustafsson and B. L. G. Jonsson, “Antenna Q and stored energy expressed in the fields, currents, and input impedance,” IEEE Trans. Antennas Propag., vol. 63, no. 1, pp. 240–249, Jan. 2015.
[29] M. Capek, L. Jelinek, and G. A. E. Vandenbosch, “Stored electromagnetic energy and quality factor of radiating structures,” Proc. Roy. Soc. A, Math., Phys. Eng. Sci., vol. 472, no. 2188, pp. 20150870, 2016.
[30] G. A. E. Vandenbosch, “Radiators in time domain—Part I: Electric, magnetic, and radiated energies,” IEEE Trans. Antennas Propag., vol. 61, no. 8, pp. 3995–4003, Aug. 2013.
[31] ——, “Radiators in time domain—Part II: Finite pulses, sinusoidal regime and Q factor,” IEEE Trans. Antennas Propag., vol. 61, no. 8, pp.
[32] M. Gustafsson and C. Ehrenborg, ‘‘State-space models and stored electromagnetic energy for antennas in dispersive and heterogeneous media,’’ Radio Sci., vol. 52, no. 11, pp. 1325–1343, 2017.
[33] G. B. Xiao, C. Xiong, S. Huang, R. Liu, Y. Hu, “A new perspective on the reactive electromagnetic energies and Q factors of antennas,” IEEE Access, vol. 8, 8999565, pp. 173790-173803, Oct. 2020.
[34] G. B. Xiao, Y. Hu and S. Xiang, “Comparison of five formulations for evaluating Q factors of antennas,” IEEE MTT-S Int. Conf. Numer. Electromagn. Multiphysics Model. Optim. (NEMO), pp. 1-3, 2020. doi: 10.1109/NEMO49486.2020.9343605.
[35] G. B. Xiao, “A theory for analysis of pulse electromagnetic radiation,” TechRxiv. Preprint. https://doi.org/10.36227/techrxiv.14054051.v4, 2021.
[36] ——, “Electromagnetic energy balance equations and Poynting theorem,” TechRxiv. Preprint. doi:10.36227/techrxiv.12555698.v1, 2020.
[37] ——, “A theory for electromagnetic radiation and coupling,” TechRxiv. Preprint. doi:10.36227/techrxiv.16686112.v2, 2021.
[38] ——, “The Schott energy and the reactive energy in electromagnetic radiation and mutual couplings.” TechRxiv. Preprint. doi:10. 36227/techrxiv. 16914235.v2,2021.
[39] Ø. Grøn, “The significance of the Schott energy for energy-momentum conservation of a radiating charge obeying the Lorentz-Abraham-Dirac equation,” Am. J. Phys., vol. 79, no. 1, pp. 115–122, 2011.
[40] T. Nakamura, “On the Schott term in the Lorentz-Abraham-Dirac equation,” Quantum Beam Sci., vol. 4, pp. 34, 2020.
[41] J. D. Jackson, “Classical Electrodynamics;” 3rd ed., John Wiley & Sons: New York, NY, USA, 1998.
[42] F. Rohrlich, “Classical Charged Particles,” 3rd ed., World Scientific Publishing: Singapore, 2007.

[43] J. A. Kong, “Fundamentals in electromagnetic wave theory,” 3rd ed., Cambridge, MA, USA: EMW Publishing, 2008, pp.65-67.
[44] X. Tian, G. B. Xiao, and S. Xiang, “Application of analytical expressions for retarded-time potentials in analyzing the transient scattering by dielectric objects,” IEEE Antennas Wireless Propag. Lett., vol.13, pp.1313-1316, 2014.
[45] S. M. Rao and D. R. Wilton, “Transient scattering by conducting surfaces of arbitrary shape,” IEEE Trans. Antennas Propag., vol. 39, no. 1, pp.56–61, Jan. 1991.
[46] S. M. Rao, D. R. Wilton, and A. W. Glisson, “Electromagnetic scattering by surfaces of arbitrary shape,” IEEE Trans. Antennas Propag., vol. 30, no. 3, pp. 409–418, Mar. 1982.